JOURNAL OF SOLID STATE CHEMISTRY **58**, 71–77 (1985)

Structural Refinements of Praseodymium and Neodymium Orthophosphate

D. F. MULLICA AND DAVID A. GROSSIE

Departments of Chemistry and Physics, Baylor University,
Waco, Texas 76798

AND L. A. BOATNER

*Solid State Division, Oak Ridge National Laboratory,**
Oak Ridge, Tennessee 37831

Received August 4, 1984; in revised form October 29, 1984

The crystal structures of $PrPO_4$ and $NdPO_4$ have been determined by single crystal X-ray diffraction techniques. The structures are isostructural with $CePO_4$ and $LaPO_4$, and are monoclinic in space group $P2_1/n$. The cell constants are $a = 6.741(3)$, $b = 6.961(4)$, $c = 6.416(3)$ Å, and $\beta = 103.63(3)°$ for $PrPO_4$ and $a = 6.722(1)$, $b = 6.933(1)$, $c = 6.390(2)$ Å, and $\beta = 103.72(2)°$ for $NdPO_4$. The least-squares structural refinements of $PrPO_4$ and $NdPO_4$ yielded R values of 0.034 and 0.038 based on 810 and 947 unique reflections, respectively. The lanthanide metal atoms are coordinated with nine oxygens and are linked together by very slightly distorted tetrahedral phosphate groups. The nine oxygen atoms ligating the lanthanide atoms form a polyhedron that is best described as a pentagonal interpenetrating tetrahedron.

Introduction

Polycrystalline ceramics formed by mixed lanthanide orthophosphates are potential hosts for the disposal of actinide and other nuclear wastes (*1–3*). Such ceramics represent synthetic analogs of the lanthanide orthophosphate mineral monazite. This mineral is a complex mixture of rare-earth orthophosphates found primarily in the first half of the lanthanide series, and it also contains relatively high (up to 10 to 15 wt%) concentrations of the actinide elements thorium and uranium. (In fact, monazite ores are the primary commercial source of thorium.) As a part of a series of continuing investigations of those properties of lanthanide orthophosphates that are relevant to their application to the problem of nuclear waste disposal, orthophosphate single crystals of every member of the transition series (except Pm) have been prepared. Additionally, single crystals of the related compounds YPO_4 and $ScPO_4$ have been grown. These single crystal specimens have been employed in studies that include EPR investigations of mixed lanthanide–actinide systems (*4*) and mixed lanthanide–

---

* Operated by Martin Marietta Energy Systems, Inc. under Contract DE-AC05-840R21400 with the U.S. Department of Energy.

0022-4596/85 $3.00

iron group impurity systems (*5–6*), optical investigations (*7–10*), and studies using Raman spectroscopy (*11*) and Rutherford backscattering (*3*). Precise structural data for these compounds were considered to be an important element in these investigations and crystallographic data for many of the subject compounds have been reported previously (*12–16*). In the case of $LaPO_4$, which has a monoclinic structure (space group $P2_1/n$) characteristic of the orthophosphates formed by the elements La to Gd, a recent coordination study has revealed that the lanthanum atom is 9-coordinated (*12*). The 9-oxygen atoms were found to form a pentagonal interpenetrating tetrahedral polyhedron (PITP). This new ninefold coordination is neither a tricapped trigonal prism (TTP) nor a monocapped square antiprism (MSAP), nor is it intermediate between TTP and MSAP. Additional evidence for this new arrangement has been provided by our recent results on the structure of $SmPO_4$, $EuPO_4$, and $GdPO_4$ (*17*). In the present work, we present structural refinements for the compounds $PrPO_4$ and $NdPO_4$, and these results are also consistent with the formation of a PITP arrangement. With the addition of the $PrPO_4$ and $NdPO_4$ refinements to our previously published work, precise structural data are now available for the entire stable lanthanide series (including $LaPO_4$ and $LuPO_4$) plus YPO_4 and $ScPO_4$.

Experimental

Single crystals of $PrPO_4$ and $NdPO_4$ were grown using a modified form (*18*) of a technique originally developed by Feigelson (*19*). The resulting specimens were selected on the basis of their optical quality and were ground into spheres with mean radii of 264 and 218.6 μm for $PrPO_4$ and $NdPO_4$, respectively. The spherical crystals were then mounted on glass fibers and transferred to the goniometer of an Enraf–Nonius CAD-4F automated diffractometer. This instrument was equipped with a dense graphite monochromator (takeoff angle, 5.8°; MoK_α, λ_{mean} = 0.71073 Å at 292 K), which is assumed to be ideally imperfect, and a lithium-doped silicon solid-state detector system. The energy dispersive analytical capability of this system was used to obtain X-ray fluorescence data for the same single crystal used in the X-ray structural refinement (*20*). The heavy lanthanide metal elements were initially verified qualitatively using the appropriate identifying L_α, L_β, and $L_{\beta 2}$ lines. The orientation matrix used for the data collection and the lattice parameters listed in Table I were determined by least-squares refinements of 25 carefully centered reflections. Intensity data were measured employing the ω–2θ scan mode in the range and scan limits listed in Table I. During the fast prescan (3.35° min^{-1}), all reflections having less than 75 counts above

TABLE I

EXPERIMENTAL AND STATISTICAL SUMMARIES FOR PRASEODYMIUM AND NEODYMIUM ORTHOPHOSPHATE

	$PrPO_4$	$NdPO_4$
a (Å)	6.741(3)	6.722(1)
b (Å)	6.961(4)	6.933(1)
c (Å)	6.416(3)	6.390(2)
β (°)	103.63(3)	103.72(2)
Crystal system	Monoclinic	Monoclinic
Space group	$P2_1/n$ (No. 14)	$P2_1/n$ (No. 14)
Z	4	4
V (Å^3)	292.6(5)	289.3(2)
MW	235.9	239.2
Dc (Mg m^{-3})	5.355	5.492
Crystal radius (mm)	0.264	0.219
μ (MoK_α) (mm^{-1})	16.96	18.385
$\Delta\omega$ (°) (ω–2θ scan)	$1.25 + 0.35 \tan \theta$	$1.25 + 0.35 \tan \theta$
$\Delta\theta$ (°)	1.5–30	1.5–27
Scan limits (°) (min^{-1})	0.38–3.35	0.38–3.35
Unique reflections	810	947
Systematic absences	$h0l$, $l + h = 2n + 1$	$h0l$, $l + h = 2n + 1$
	$0k0$, $k = 2n + 1$	$0k0$, $k = 2n + 1$
R	0.034	0.038
R_w	0.035	0.039
Gnft (Σ_2)	2.40	2.35
$g(e^{-2})$ (10^{-6})	4.04(4)	3.28(4)
Max[$\Delta - \xi_i/\sigma(\xi_i)$] ($10^{-3}$)	1.1	4.1
Residual ρ (e Å^{-3})	Max 3.1(4)	3.5(6)
	Min −2.2(4)	−4.2(6)

background were assumed to be unobserved. Selected standard reflections ($1\,\bar{3}\,\bar{2}$ and $\bar{3}\,2\,6$ for $PrPO_4$ and $0\,\bar{1}\,\bar{2}$ and $\bar{2}\,0\,2$ for $NdPO_4$) were monitored every 2 hr of data collection. Examination of each set of standards revealed only random variations (<1.2 and <0.5%, respectively). corrections were made for Lorentz and polarization effects. Spherical absorption corrections ($\mu R = 4.48$ and 4.02 for $PrPO_4$ and $NdPO_4$, respectively) were also applied to each data set according to Bond (*21*). Standard deviations of the structure factors were computed as $\sigma(|F_0|) = 0.5\ (\mathrm{VLp})^{1/2}\ [(\mathrm{Pk} + \mathrm{Bg} + p^2 I_{\mathrm{rel}}^2)/I_{\mathrm{rel}}]^{1/2}$, where VLp is the standard Lorentz-polarization term, Pk is the peak intensity, Bg is the sum of the background counts taken on both sides of the peak, p is the ignorance factor (0.02 in this work), and I_{rel} is Pk–Bg. All data with $I_{\mathrm{rel}} > 3\sigma\ (I_{\mathrm{rel}})$ were used in the solution and refinement of the structures. Examination of the observed data revealed systematic extinctions consistent with space group $P2_1/n$. After averaging redundant data, 810 and 947 reflections for $PrPO_4$ and $NdPO_4$ were found to be unique (averaging residuals of 0.020 and 0.017). The crystal data, experimental conditions, and statistical summaries are presented in Table I.

Structural Refinement

The final atomic coordinates obtained for isostructural lanthanum orthophosphate (*12*) were used as initial positional parameters for the refinement of the current structures. These positions were refined employing a full-matrix least-squares program (*22*). After several cycles in which the anisotropic thermal parameters were varied and secondary extinction corrections ($g \times 10^{-6}\ e^{-2}$) were applied, the R factors stabilized with maximum shift/error values less than 0.005 (see Table I). The residual and weighted indices used in the refinement are defined as $R = \Sigma\Delta F/\Sigma|F_0|$ and $R_w = [\Sigma w(\Delta F)^2/\Sigma w|F_0|^2]^{1/2}$ where $\Delta F = ||F_0| - |F_c||$. The weighting factors were defined as the reciprocals of the square of the standard deviation on $|F|$, i.e., $w = \sigma^{-2}(|F|_0)$. The minimized quantity was $\Sigma w||F_0| - |F_c||^2$. In the final least-squares cycle refinement for $PrPO_4$ and $NdPO_4$, the maximum respective values of abscission, defined as $[\Delta\xi i/\sigma(\xi i)]$ where ξi values are varied parameters, were 0.0011 and 0.0041, respectively. Some residual density was observed in the vicinity of the praseodymium and neodymium atoms in each of the final difference Fourier maps. This is not unusual in the case of heavy metals like the lanthanides. Elsewhere, the difference Fourier map was virtually featureless, and revealed only a random undulating background. Atomic scattering factors and anomalous dispersion correction factors for all atoms were taken from the International Tables (*23*). Atomic coordinates and thermal parameters along with the bond distances and angles are given in Tables II,[1] III, and IV.

Discussion

Figure 1 presents an ORTEP stereo drawing of monoclinic ($P2_1/n$) $NdPO_4$. This 9-coordinated geometric system is best described as a pentagonal interpenetrating tetrahedral polyhedron (PITP) with a point group symbol of C_s (see Fig. 2). A full discussion has been presented in a recent structural paper (*12*) describing the 9-coordinated geometry for analogs to the mono-

---

[1] See NAPS document No. 04256 for 22 pages of supplementary material. Order from ASIS/NAPS, Microfiche Publications, P.O. Box 3513, Grand Central Station, New York, NY 10163. Remit in advance \$4.00 for microfiche copy or for photocopy, \$7.75 up to 20 pages plus \$.30 for each additional page. All orders must be prepaid. Institutions and organizations may order by purchase order. However, there is a billing and handling charge for this service of \$15. Foreign orders add \$4.50 for postage and handling, for the first 20 pages, and \$1.00 for additional 10 pages of material. Remit \$1.50 for postage of any microfiche orders.

TABLE II

ATOMIC POSITIONAL PARAMETERS (× 10^4) AND EQUIVALENT ISOTROPIC THERMAL PARAMETERS (× 10^4) FOR PRASEODYMIUM AND NEODYMIUM ORTHOPHOSPHATE

Atom	x	y	z	U_{eq}[a]
$PrPO_4$				
Pr[b]	28164(5)	15864(5)	9982(5)	33(1)
P	3046(3)	1628(2)	6131(3)	47(3)
O(1)	2518(8)	34(8)	4470(8)	115(11)
O(2)	3807(7)	3316(7)	4983(8)	80(10)
O(3)	4744(7)	1046(7)	8052(8)	70(10)
O(4)	1248(7)	2161(7)	7127(8)	57(10)
$NdPO_4$				
Nd[b]	28184(5)	15803(5)	9950(6)	25(1)
P	3037(3)	1629(3)	6127(3)	32(3)
O(1)	2502(8)	37(9)	4437(9)	66(11)
O(2)	3812(8)	3329(8)	4985(9)	59(11)
O(3)	4739(9)	1055(9)	8078(9)	71(11)
O(4)	1245(8)	2139(8)	7120(10)	74(11)

[a] U_{eq} defined as one-third the trace of the orthogonalized U_{ij} tensor.

[b] coordinates × 10^5.

TABLE III

ANISOTROPIC THERMAL PARAMETERS (× 10^4) FOR PRASEODYMIUM AND NEODYMIUM ORTHOPHOSPHATE

Name	$U(1,1)$	$U(2,2)$	$U(3,3)$	$U(1,2)$	$U(1,3)$	$U(2,3)$
$PrPO_4$						
Pr	16(1)	7(1)	73(1)	1(1)	3(1)	6(1)
P	17(6)	36(7)	83(7)	−2(5)	1(5)	2(5)
O(1)	100(20)	141(24)	74(19)	31(19)	−43(17)	48(18)
O(2)	72(18)	42(20)	137(20)	−22(16)	43(15)	26(17)
O(3)	57(18)	67(19)	80(19)	29(17)	4(15)	15(17)
O(4)	47(17)	−4(17)	174(20)	75(16)	30(15)	9(17)
$NdPO_4$						
Nd	8(1)	8(1)	47(1)	2(1)	−18(1)	6(1)
P	11(6)	17(7)	56(7)	1(6)	−14(5)	−2(6)
O(1)	50(20)	78(23)	37(20)	32(18)	−53(18)	33(18)
O(2)	25(19)	58(21)	89(20)	−13(18)	3(16)	17(19)
O(3)	40(20)	71(22)	88(21)	32(18)	−13(17)	14(19)
O(4)	63(20)	19(20)	141(23)	37(18)	27(18)	−10(20)

Note: The form of the anisotropic thermal parameter is exp $[-2\pi^2\{h^2a^{*2}U(1,1) + k^2b^{*2}U(2,2) + l^2c^{*2}U(3,3) + 2hka^*b^*U(1,2) + 2hla^*c^*U(1,3) + 2klb^*c^*U(2,3)\}]$.

clinic monazite structure (MXO_4), where M atoms are the lighter members of the lanthanide series and the X atom is phosphorus, but could conceivably be V or As. In the past, a 9-coordinated system has been characterized as a tricapped trigonal prism (TTP), a monocapped square antiprism (MSAP), or a severely distorted intermediate between TTP and MSAP. There is a close interrelationship between the two idealized geometries, TTP and MSAP (*24, 25*). The MSAP (C_{4v}) can be generated from the ideal TTP (D_{3h}) by slightly elongating one of the edges of the trigonal prism thereby producing a distortion between the

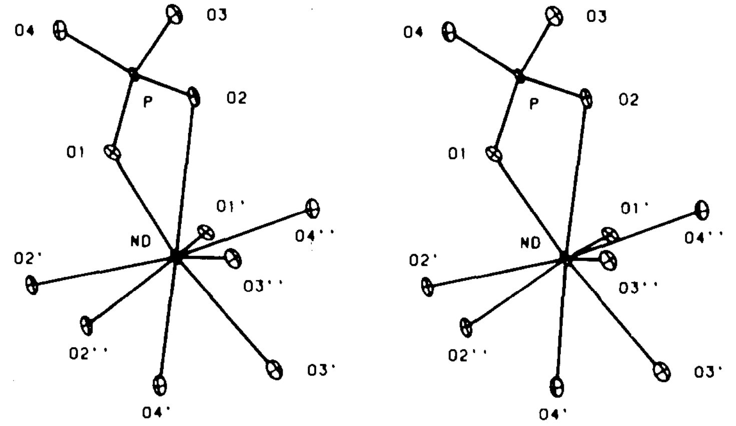

FIG. 1. Stereoscopic drawing of the Nd and P coordination polyhedra in monoclinic ($P2_1/n$) $NdPO_4$ with the labeling and number scheme (PITP, pentagonal interpenetrating tetrahedral polyhedron).

TABLE IV

SELECTED BOND DISTANCES (Å) AND ANGLES (°) FOR PRASEODYMIUM AND NEODYMIUM ORTHOPHOSPHATE

	$PrPO_4$	$NdPO_4$		$PrPO_4$	$NdPO_4$
Ln–O(1)[a]	2.526(3)	2.500(4)	P–O(1)	1.522(4)	1.526(4)
	2.423(4)	2.416(4)	P–O(2)	1.537(3)	1.540(4)
			P–O(3)	1.526(3)	1.531(4)
			P–O(4)	1.543(3)	1.530(4)
Ln–O(2)	2.628(3)	2.617(4)			
	2.540(3)	2.520(4)	Av	1.532	1.532
	2.762(3)	2.759(4)			
			O(1)–P–O(2)	105.7(2)	105.5(2)
Ln–O(3)	2.442(3)	2.434(4)			
	2.561(3)	2.533(4)	O(1)–P–O(3)	112.3(2)	113.2(2)
Ln–O(4)	2.492(3)	2.481(4)	O(1)–P–O(4)	112.9(2)	112.6(2)
	2.418(3)	2.414(4)			
			O(2)–P–O(3)	108.6(2)	108.6(2)
O(1)–O(2)	2.439(5)	2.441(5)			
O(1)–O(3)	2.531(5)	2.552(5)	O(2)–P–O(4)	113.5(2)	114.0(2)
O(1)–O(4)	2.553(5)	2.542(5)			
O(2)–O(3)	2.488(5)	2.489(5)	O(3)–P–O(4)	104.0(2)	103.4(2)
O(2)–O(4)	2.575(5)	2.576(5)			
O(3)–O(4)	2.419(4)	2.403(5)	Av	109.5	109.6

[a] Estimated standard deviations are given in parentheses.

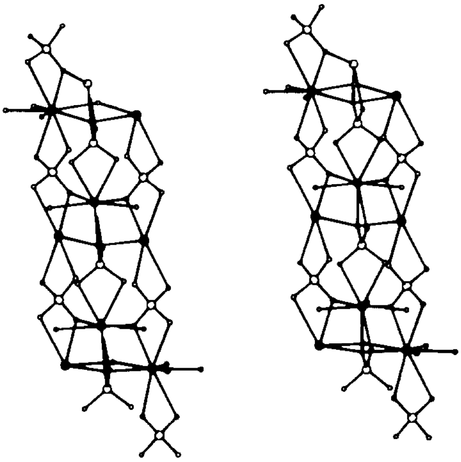

FIG. 3. Stereoview of the interlocking arrangement of the chain-like strands in monoclinic $LnPO_4$. (Large filled-in atoms are *Ln* elements, large open circles represent phosphorus atoms, and small open circles represent oxygen atoms.)

parallel apical trigonal planes. Parallelism is lost and the interplanar angle generated is 15.7°. Therefore, the dihedral angle between the apical planes is an important factor for evaluating whether a geometry is a distorted TTP ($\leqslant 15.7°$) or is another idealized geometry, MSAP ($\simeq 15.7°$). Parallelism exists between the square anti-prism planes of the MSAP polyhedron. The dihedral angle between these planes also plays an important role in deciding whether a 9-coordinated system can be classified as a MSAP or a distorted MSAP ($\leqslant 15°$). If the dihedral angle is greater than 15° ($\geqslant 10°$), and a new geometry can be characterized, the term distorted MSAP must be abandoned. (This is particularly true when a new point group symmetry is observed.) The dihedral angles involved in the case of $PrPO_4$ or $NdPO_4$ are 19.3 and 19.2°, respectively (see Ref. (*12*) for complete details).

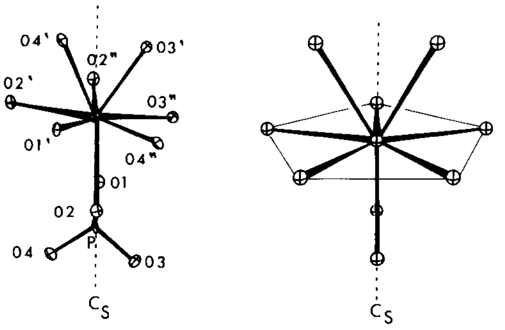

FIG. 2. (a) $NdPO_4$—PITP structurally oriented to show C_s symmetry. (b) Idealized PITP demonstrating the plane of symmetry, C_s.

The rigidity associated with the PITP geometry of these monoclinic lanthanide orthophosphates and conceivably other monazite type compounds is attributed to the bidentate type bonding of the tetrahedral phosphate groups. In ninefold coordination, the lanthanide atoms are apically connected in a chain-like manner by very slightly distorted tetrahedral phosphate groups, see Fig. 3. The apical bidentate type bonding accounts for four of the nine oxygen atoms in the nine-coordinated polyhedron. The five remaining equatorial oxygen atoms which form the pentagonal plane of the polyhedron are bridged to five surrounding chain-like strands. The bridging provides a locking effect that secures and supports the pentagonal plane. Negligible torsion effects attributed to the locking "device" are observed in the pentagonal plane. After applying a least-squares planarity program (*26*) the resulting conclusion related to the atoms defining the pentagonal plane is that planarity exists with negligible torsion. For simplicity and clarity, the stereoview of the interlocking mechanism shown in Fig. 3, displays only two surrounding strands instead of five. It is apparent that more than two strands would confuse rather than clarify the situation. Note the 9-coordinated geometry of monoclinic $Ln\mathrm{PO}_4$ in the lower right portion of the stereo drawing in Fig. 3 (with small filled in oxygen atoms) and the two centrally located ninefold *Ln* atoms displaying the locking effect.

Future experimental investigations and literature surveys of related systems are expected to lend additional supporting evidence for the new ninefold coordination geometry (PITP). With the addition of the structural refinements presented here to our previously published work, structural data now exist for the complete lanthanide series plus ScPO_4 and YPO_4.

Acknowledgments

The authors gratefully acknowledge the financial support of this work, in part, by The Robert A. Welch Foundation (Grant AA-668) and Baylor University. The authors also acknowledge with sincere and genuine thankfulness the unrelenting assistance and support of our departed friend Dr. W. O. Milligan who was an integral part of our research program.

References

1. L. A. Boatner, G. W. Beall, M. M. Abraham, C. B. Finch, P. G. Huray, and M. Rappaz, *in* "Scientific Basis for Nuclear Waste Management," (C. J. Northrup, Ed.), Vol. 2, p. 289, Plenum, New York (1980).
2. L. A. Boatner, G. W. Beall, M. M. Abraham, C. B. Finch, R. J. Floran, P. G. Huray, and M. Rappaz, "Management of Alpha-Contaminated Wastes," IAEA-SM-246/73, p. 411. International Atomic Energy Agency, Vienna (1981).
3. B. C. Sales, C. W. White, and L. A. Boatner, *Nucl. Chem. Waste Manage.* **4,** (1984).
4. M. M. Abraham and L. A. Boatner, *Phys. Rev. B* **26,** 1434 (1982).
5. M. Rappaz, M. M. Abraham, J. O. Ramey, and L. A. Boatner, *Phys. Rev. B* **23,** 1012 (1981).
6. M. M. Abraham, L. A. Boatner, J. O. Ramey, and M. Rappaz, *J. Chem. Phys.* **78,** 3 (1983).
7. K. L. Kelley, G. W. Beall, J. P. Young, and L. A. Boatner, "Scientific Basis for Nuclear Waste Management" (John G. Moore, Ed.), Vol. 3, pp. 189–195. Plenum, New York (1981).
8. T. Hayhurst, S. Shalimoff, N. Edelstein, L. A. Boatner, and M. M. Abraham, *J. Chem. Phys.* **74,** 5449 (1981).
9. T. Hayhurst, S. Shalimoff, J. G. Conway, N. Edelstein, L. A. Boatner, and M. M. Abraham, *J. Chem. Phys.* **76,** 3960 (1982).
10. P. C. Becker, T. Hayhurst, G. Shalimoff, J. G. Conway, L. A. Boatner, and M. M. Abraham, *J. Chem. Phys.*, in press.
11. G. M. Begun, G. W. Beall, L. A. Boatner, and W. T. Gregor, *J. Raman Spectrosc.* **11,** 273 (1981).
12. D. F. Mullica, W. O. Milligan, David A. Grossie, G. W. Beall, and L. A. Boatner, *Inorg. Chim. Acta* **95,** 231 (1984).
13. W. O. Milligan, D. F. Mullica, G. W. Beall, and L. A. Boatner, *Inorg. Chim. Acta* **60,** 39 (1982).
14. G. W. Beall, L. A. Boatner, D. F. Mullica, and W. O. Milligan, *J. Inorg. Nucl. Chem.* **43,** 101 (1981).
15. W. O. Milligan, D. F. Mullica, G. W. Beall, and L. A. Boatner, *Acta Crystallogr. C* **39,** 23–24 (1983).
16. W. O. Milligan, D. F. Mullica, G. W. Beall, and L. A. Boatner, *Inorg. Chim. Acta* **70,** 133 (1983).
17. D. F. Mullica, David A. Grossie, G. W. Beall, and L. A. Boatner, "Inorganica Chimica Acta—f-Block Elements," in press.
18. M. Rappaz, J. O. Ramey, L. A. Boatner, and M. M. Abraham, *J. Chem. Phys. I* **76,** 40 (1982).
19. R. S. Feigelson, *J. Amer. Ceram. Soc.* **47,** 257 (1964).
20. D. F. Mullica, G. W. Beall, W. O. Milligan, and J. D. Oliver, *J. Appl. Crystallogr.* **12,** 263 (1979).

21. W. L. Bond, "International Tables for X-ray Crystallography," Vol. II, p. 302, Kynoch Press, Birmingham, England (1962).
22. Enraf-Nonius, "ENRAF-NONIUS VAX Structure Determination Package," Delft (1982).
23. J. A. Ibers and W. C. Hamilton, "International Tables for X-Ray Crystallography," Vol. IV, p. 72, Kynoch Press, Birmingham (1974).
24. L. J. Guggenberger and E. L. Muetterties, *J. Amer. Chem. Soc.* **98,** 7221 (1976).
25. B. E. Robertson, *Inorg. Chem.* **16,** 2735 (1977).
26. D. M. Blow, *Acta Crystallogr.* **13,** 168 (1960).